

## Effect of the erbium dopant architecture on the femtosecond relaxation dynamics of silicon nanocrystals

A. C. S. Samia, Y. Lou, C. Burda, R. A. Senter, and J. L. Coffey

Citation: *The Journal of Chemical Physics* **120**, 8716 (2004); doi: 10.1063/1.1695318

View online: <http://dx.doi.org/10.1063/1.1695318>

View Table of Contents: <http://scitation.aip.org/content/aip/journal/jcp/120/18?ver=pdfcov>

Published by the [AIP Publishing](#)

---

### Articles you may be interested in

[Dopant effects on the photoluminescence of interstitial-related centers in ion implanted silicon](#)

*J. Appl. Phys.* **111**, 094910 (2012); 10.1063/1.4710991

[Dopant effects on solid phase epitaxy in silicon and germanium](#)

*J. Appl. Phys.* **111**, 034906 (2012); 10.1063/1.3682532

[Relaxation dynamics in photoexcited GaSe nanoparticles](#)

*J. Chem. Phys.* **117**, 8944 (2002); 10.1063/1.1513454

[Role of the energy transfer in the optical properties of undoped and Er-doped interacting Si nanocrystals](#)

*J. Appl. Phys.* **89**, 264 (2001); 10.1063/1.1331074

[High-energy ion-implantation-induced gettering of copper in silicon beyond the projected ion range: The trans-projected-range effect](#)

*J. Appl. Phys.* **88**, 5645 (2000); 10.1063/1.1316054

---



# Effect of the erbium dopant architecture on the femtosecond relaxation dynamics of silicon nanocrystals

A. C. S. Samia, Y. Lou, and C. Burda<sup>a)</sup>

*Center for Chemical Dynamics and Nanomaterials Research, Department of Chemistry, Case Western Reserve University, Cleveland, Ohio 44106*

R. A. Senter and J. L. Coffey<sup>b)</sup>

*Department of Chemistry, Texas Christian University, Ft. Worth, Texas 76129*

(Received 17 September 2003; accepted 12 February 2004)

Femtosecond pump–probe absorption spectroscopy is used to investigate the role of  $\text{Er}^{3+}$  dopants in the early relaxation pathways of photoexcited Si nanocrystals. The fate of photoexcited electrons in three different Si nanostructures was studied and correlated with the effect of Er-doping and the nature of the dopant architecture. In Si nanocrystals without  $\text{Er}^{3+}$  dopant, a trapping component was identified to be a major electron relaxation mechanism. Addition of  $\text{Er}^{3+}$  ions into the core or surface shell of the nanocrystals was found to open up additional nonradiative relaxation pathways, which is attributed to Er-induced trap states in the Si host. Analysis of the photodynamics of the Si nanocrystal samples reveals an electron trapping mechanism involving trap-to-trap hopping in the doped nanocrystals, whereby the density of deep traps seem to increase with the presence of erbium. To gain additional insights on the relative depths of the trapping sites on the investigated nanostructures, benzoquinone was used as a surface adsorbed electron acceptor to facilitate photoinduced electron transfer across the nanocrystal surface and subsequently assist in back electron transfer. The established reduction potential ( $-0.45$  V versus SCE) of the electron acceptor helped reveal that the erbium-doped nanocrystal samples have deeper trapping sites than the undoped Si. Furthermore, the measurements indicate that internally Er-doped Si have relatively deeper trapping sites than the erbium surface-enriched nanocrystals. The electron-shuttling experiment also reveals that the back electron transfer seems not to recover completely to the ground state in the doped Si nanocrystals, which is explained by a mechanism whereby the electrons are captured by deep trapping sites induced by erbium addition in the Si lattice. © 2004 American Institute of Physics. [DOI: 10.1063/1.1695318]

## I. INTRODUCTION

The implantation of  $\text{Er}^{3+}$  ions into silicon is an important aspect in the fabrication of near IR light emitting diodes and the associated optoelectronic components compatible with available silicon technology.<sup>1–4</sup> This combination is of great interest because of the synergism between the 1540 nm emission from the erbium centers and the maximum transmission window of a silica-based waveguide.<sup>5,6</sup> In the case of erbium implanted into bulk crystalline Si, it appears that a strongly competitive Auger pathway reduces the emission intensity at room temperature,<sup>7,8</sup> thereby diminishing its potential usefulness in optoelectronic platforms. However, the introduction of  $\text{Er}^{3+}$  ions into nanometer sized Si is one possible route to suppress such competitive pathways.<sup>3,4,9–12</sup> Since bulk Si is an indirect bandgap material, lattice vibrations (phonons) are needed to moderate the radiative recombination of an electron and hole in order to conserve momentum. Therefore, this process is very inefficient and low quantum efficiencies of  $10^{-4}\%$  are achieved at room temperature.<sup>13</sup> However, when carriers are quantum confined, their wave functions spread out in momentum space

and the band structure is believed to become more “direct-like” in nature. Thus, making the recombination process more efficient and quantum efficiencies of up to 1%–10% are achievable.<sup>9–14</sup> Furthermore, it has been shown that when selected active impurities are inserted in the Si lattice, room temperature light emission can be observed.<sup>13,14</sup> In the case of Si nanoclusters embedded in bulk  $\text{SiO}_2$ , the excitation of  $\text{Er}^{3+}$  using pump wavelengths that do not correspond to any of the principal  $\text{Er}^{3+}$  bands is observed.<sup>3,15</sup> This coupling mechanism is very important since it relaxes the requirements on the  $\text{Er}^{3+}$  pump wavelength leading to the production of pumpable broad-band optical amplifiers at the important telecommunications wavelength of 1540 nm.

Because of the great potential of nanometer sized Si for optoelectronic applications, we have been extensively investigating the “bottom-up” synthesis of nanocrystals of this material doped with the rare-earth element erbium ( $\text{Er}^{3+}$ ) along with their resulting structure and photophysical properties.<sup>16–21</sup> In terms of dopant location, two different types of particles can be prepared with the erbium centers in two different coordination environment: Nanocrystals with  $\text{Er}^{3+}$  randomly dispersed throughout the crystal,<sup>16,17,19–21</sup> and nanocrystals whereby the  $\text{Er}^{3+}$  centers are preferentially enriched at the surface.<sup>18,21</sup> For the former, the characteristic

<sup>a)</sup>Electronic mail: burda@cwru.edu

<sup>b)</sup>Electronic mail: j.coffey@tcu.edu

1540 nm emission associated with the rare earth ion is detected via a pathway that involves energy transfer from the Si exciton to the rare earth ligand field transition(s).<sup>16</sup> In the latter case, it is significant to note that the as-formed erbium surface-enriched Si nanocrystals are effectively nonluminescent and only emit with a direct ligand field excitation mechanism following a brief high temperature anneal at 800 °C.<sup>18</sup>

In both of the above systems, a crucial feature of their photophysical properties relevant to emission, specifically the initial dynamics of the photogenerated charge carriers, is still lacking at present. Even in well passivated and dislocation free Si nanocrystals, the luminescence lifetimes are very long ( $\mu\text{s}$ -ms at room temperature) thereby exposing the radiative process to strong competition with fast nonradiative recombination pathways.<sup>13</sup> Thus, a better understanding of the nonradiative carrier relaxation pathways in silicon nanocrystals is important in optimizing the emission properties of Si for optoelectronic applications.

Studies of the ultrafast dynamics of optically generated charge carriers have been previously shown to be informative with respect to a range of semiconducting silicon materials, including hydrogenated amorphous Si (a-Si:H)<sup>22,23</sup> as well as porous Si.<sup>24–26</sup> We have employed femtosecond time-resolved pump-probe spectroscopy to study the nonradiative relaxation dynamics of the conduction band electrons in undoped silicon nanocrystals, randomly dispersed Er-doped silicon nanocrystals, and erbium surface-enriched silicon nanocrystals. Using ultrafast pump-probe spectroscopy we investigated the influence of dopant architecture on the initial carrier dynamics of erbium-doped silicon nanocrystals. To gain insights on the relative depths of the trapping sites on the investigated Si nanostructures, benzoquinone was used as a surface adsorbed electron acceptor to facilitate the photo-induced electron transfer across the nanocrystal surface and subsequently assist in back electron transfer.

## II. EXPERIMENT

### A. Nanocrystal synthesis

Nanocrystals of randomly dispersed Er-doped Si were prepared according to a previously reported procedure.<sup>16</sup> Diluted 0.48% Si<sub>2</sub>H<sub>6</sub> (He balanced, Praxair) was pyrolyzed in the presence of the erbium CVD source compound, Er(tmhd)<sub>3</sub> vapor (Strem), which is flowed through a small pyrolysis oven (6 cm in length) that operates at 1000 °C. After a reaction period of 24 hrs, the desired nanocrystals were collected in an ethylene glycol bubbler and purified by a series of centrifugation, washing, and precipitation steps. As a control material, undoped Si nanocrystals were also prepared by employing identical reaction conditions during synthesis, except for the deliberate absence of the erbium source compound. For the preparation of erbium surface-enriched nanocrystals, the reactor was modified to decouple the Si nucleation and growth steps from the erbium incorporation event.<sup>18</sup> After the pyrolysis of the diluted disilane in a 6 cm pyrolysis oven (again operating at 1000 °C), the aerosol is mixed with Er(tmhd)<sub>3</sub> vapor (Strem) in He carrier gas (Praxair, UHP grade). Approximately 4 cm from the intro-

duction of the erbium precursor the aerosol is again heated at temperatures ranging from 750–900 °C with a small oven. Similarly, the erbium surface-enriched nanocrystals were collected as an ethylene glycol colloid and purified using the same series of steps adapted for the other nanocrystals.

All of the Si nanocrystals were structurally characterized by a combination of high-resolution transmission electron microscopy (HRTEM), selected area electron diffraction (SAED), energy dispersive x-ray analysis (EDX), and extended x-ray absorption fine structure methods (EXAFS).<sup>21</sup>

### B. Spectroscopic measurements

Femtosecond time-resolved transient absorption spectra were recorded on a Clark MXR CPA 2001 femtosecond laser system that entails an amplified erbium-doped fiber laser, which is frequency doubled to 780 nm and amplified in a regenerative amplifier. This laser set-up produces highly stable laser pulses with 120 fs full width at half maximum (FWHM) duration and 800  $\mu\text{J}$  output energy per pulse at a repetition rate of 1 kHz. A small portion of the fundamental output pulse train is used to generate white light in a 2 mm sapphire crystal while the remaining laser light is used to frequency-double the fundamental to achieve 390 nm excitation light. The excitation beam is modulated by a chopper with a 100 Hz frequency. On the other hand, the probe light is guided into a spectroscope via reflective optics in order to avoid the white light dispersion in quartz lenses. During sample measurement, the excitation beam is focused to a spot diameter of 500  $\mu\text{m}$  and the probe beam to 100  $\mu\text{m}$ . A quartz cuvette of 2 mm path length is used for the nanocrystal solutions and the sample is continuously stirred by a cell stirrer to avoid permanent bleaching of a single volume element in the solution. The pump-probe experiments are all carried out at ambient temperature. LabView-assisted data acquisition results in a “dynamics matrix” (spectra versus delay time), which is analyzed by single-value decomposition method. Global analysis of the dynamics matrix also facilitates the extraction of the significant dynamic components with high reliability, as opposed to a kinetic fit at individual wavelengths.

## III. RESULTS

### A. Characterization of Si nanocrystals

A TEM image of an Er-doped Si nanocrystal sample is shown in Fig. 1(b). The SAED pattern [inset Fig. 1(b)] is consistent with the diamond cubic phase of Si, and confirms the absence of a second phase formation with the incorporation of Er<sup>3+</sup> ions. Furthermore, previous structural analyses by HRTEM confirm the presence of defects such as dislocations and stacking faults in the nanocrystals.<sup>16</sup> This suggests that Er<sup>3+</sup> inclusion in the Si lattice may be responsible for some of the defect formation. It is interesting to note that the control sample of homogenous Si nanocrystals [Fig. 1(a)], which was synthesized by a similar method, was also found to exhibit stacking faults and other defects. However, it is important to stress, that there is a clear structural difference induced by Er<sup>3+</sup> in the doped nanocrystals, as the SAED rings in the rare-earth doped Si sample are significantly

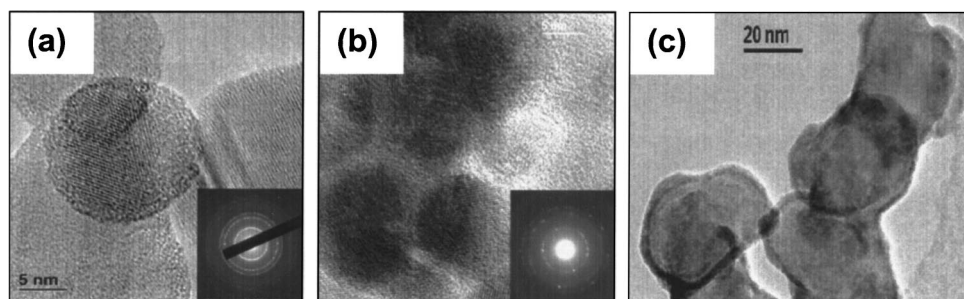


FIG. 1. HRTEM micrograph of a randomly dispersed Er-doped Si nanocrystal sample with an average size of 5 nm; the inset shows the SAED pattern of the nanocrystals. (a) High resolution TEM image of undoped Si nanocrystals along with the associated selected area electron diffraction (SAED) pattern as an inset, which is consistent with a cubic phase structure; (b) high resolution TEM image of randomly dispersed Er-doped Si nanocrystals with the inset showing a more diffuse, less-resolved SAED pattern, but is still consistent with the cubic phase structure; (c) TEM image of Er surface-enriched Si nanocrystals where a magnification is selected in which the higher Z contrast Er is evident along the surface of the nanocrystals.

broad, more diffused and less-resolved (Fig. 1). This observation supports the idea that  $\text{Er}^{3+}$  incorporation impacts the nature of defect formation within the Si nanocrystals.<sup>16</sup>

In comparison to the bright-field HRTEM image of the Er-doped Si nanoparticulate sample, the TEM image of the erbium surface-enriched nanocrystals exhibit a contrast enhancement at the outer shell, which is attributed to the clustering of erbium on the particle surface<sup>18</sup> [Fig. 1(c)]. For both nanocrystal samples, EDX and EXAFS measurements confirm Er addition to the Si nanocrystal overall, with  $\sim 2\%$  erbium dopant in the doped nanocrystals, and about 4.6% in the core-shell system.

## B Femtosecond time-resolved spectroscopy

### 1. Undoped silicon nanocrystals (Si NCs)

Following light excitation at 390 nm with 120 fs laser pulses, the undoped Si NCs show a broad, featureless transient absorption, which extends over the whole visible range. This is indicative of the indirect band gap excitation of Si.<sup>27</sup> The transient absorption, shown in Fig. 2, is extremely weak and decays exponentially with a 134 ps time constant. This rather long-lived transient is attributed to trap state absorption, which reflects the population and depopulation of defect sites in the Si NCs.

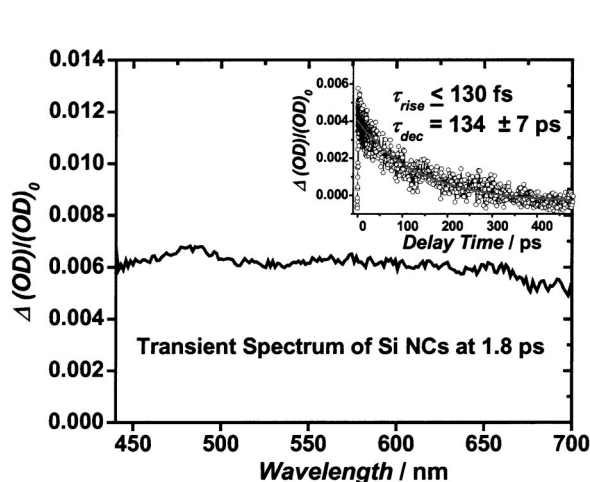


FIG. 2. Femtosecond transient absorption of Si NCs after excitation with 390 nm pulses (120 fs duration). The inset shows the kinetics observed for the transient absorption at 600 nm.

In order to assess the relative depth of the trapping site in the investigated Si nanocrystals, 1,4-benzoquinone (BQ) was added to the Si sample. From previous studies it has been shown that quinones adsorbed on semiconductor nanocrystals facilitate photoinduced electron transfer across the NC surface and subsequently assist in back electron transfer.<sup>28,29</sup> This electron shuttling process is usually faster than the inherent electron-hole recombination in the semiconductor alone.<sup>28</sup> The quinone bypasses the semiconductor core and surface trap states and shuttles the electron from the conduction band to the hole in the NC.

The femtosecond transient spectrum of Si with BQ shows the presence of an absorption between 476 and 588 nm, in addition to a bleach at 600 nm (Fig. 3). The transient absorption fits to the published absorption for the benzoquinone anion<sup>30</sup> and the transient bleach can be attributed to the positively charged nanocrystals formed after the electron transfer to the surface-adsorbed electron acceptor. By exciting an electron from the valence band and quickly extracting the excited electron with BQ, one introduces a transient p-doping into the NC, which results in the observed transient bleach.<sup>24,25,29</sup> In effect, the transient spectra are superpositions of the NC bleach and the BQ anion absorption.

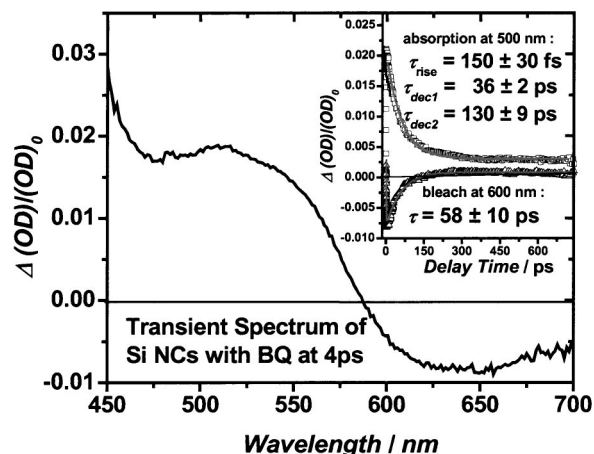


FIG. 3. Femtosecond transient spectrum of undoped Si NCs with BQ adsorbed on the surface after excitation with 390 nm pulses (120 fs duration). The inset shows the kinetics observed for the transient absorption at 500 nm and the transient bleach at 600 nm.

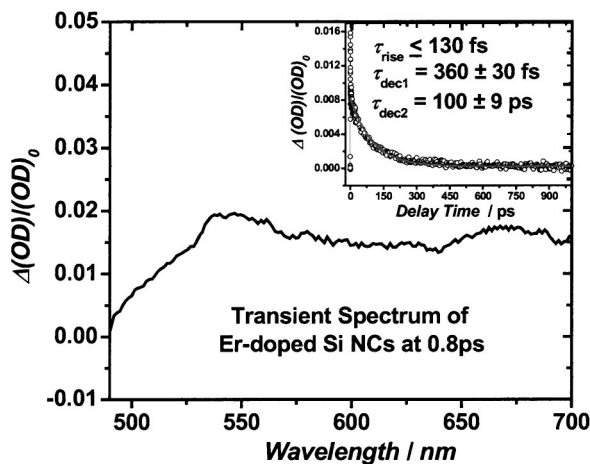


FIG. 4. Femtosecond transient absorption of Si NCs with randomly dispersed  $\text{Er}^{3+}$  dopant centers after excitation with 390 nm pulses. The inset shows the kinetics observed for the transient absorption at 610 nm.

Upon femtosecond laser excitation, the transient absorption of the  $\text{BQ}^-$  radical anion appears within 150 fs with a maximum at 500 nm. At longer wavelengths a bleach is initially observed. It is interesting to note that the formation time of the radical anion absorption was determined to be similar to the formation time observed for the Si NC bleach at 600 nm (inset, Fig. 3). The time average of the best fit for the decay of the radical ion 75 ps matches the recovery of the one for the bleach ( $\tau = 58 \pm 10$  ps). As the electron undergoes back transfer, the 500 nm absorption decays and the bleach does so as well. This suggests that the BQ acts as an electron shuttle by facilitating the withdrawal of the electron from the conduction band and the delivery to the hole in the valence band.

## 2. Randomly dispersed Er-doped Si NCs

Si NCs with randomly dispersed  $\text{Er}^{3+}$  dopants initially show a similar broad absorption band, which is quickly reduced by a fast component with a lifetime of 360 fs (Fig. 4). This spectral feature is assigned to a trapping component, which is much faster than the trapping process in the undoped Si nanocrystals previously discussed. A second trapping component is also observed with trap state lifetime of 100 ps. The transient absorption features of the trap state differ from that of the undoped Si nanocrystals, with maxima at 550 and 670 nm and the occurrence of two trapping processes.

After the addition of BQ, laser excitation leads to fast interfacial electron transfer forming the  $\text{Er-doped Si}^+\text{BQ}^-$  ion pair. The corresponding charge transfer spectrum in Fig. 5 is characterized by the superposition of the features of the BQ anion at 450–500 nm and the bleach, which is caused by the missing electron (transient p-doping) on the NC. The electron transfer time is determined to be 220 fs and the weighted charge transfer state lifetime is found to be 82.5 ps (Fig. 5). A long-lived residual absorption is also observed and can be assigned to the electrons that become localized in the trapping sites caused by the randomly dispersed  $\text{Er}^{3+}$  ions. In addition to the fast decay dynamics, the back elec-

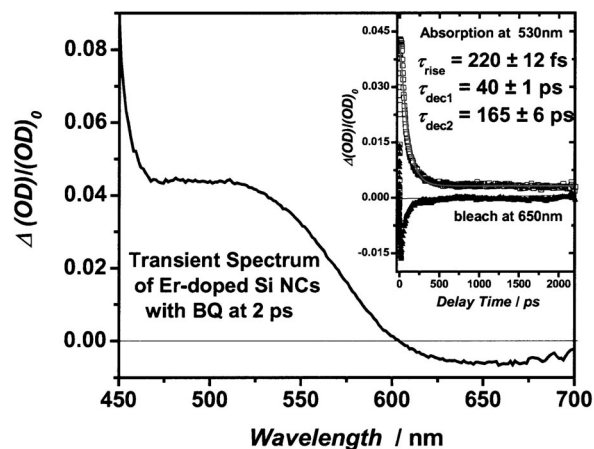


FIG. 5. Femtosecond transient absorption of randomly dispersed (RD)  $\text{Er}^{3+}$ -doped Si NCs with BQ adsorbed on the surface after excitation with 390 nm pulses (120 fs duration). The inset shows the kinetics observed for the transient absorption at 530 nm and the transient bleach at 650 nm.

tron transfer seems not to recover completely to the ground state in contrast to the undoped Si NCs. Instead of the electron–hole recombination, which would lead to the decay of any transient spectrum, a long-lived transient absorption is observed. This could be explained by a mechanism in which the electrons are captured by  $\text{Er}^{3+}$ -related trapping sites hindering the complete recovery of the NC ground state. However, it seems that the undoped Si NCs described above also have low enough trapping sites available to intercept the electron–hole recombination process, consistent with the stacking faults pointed out in Fig. 1.

Overall, it appears that the internal  $\text{Er}^{3+}$  ions are more efficient trapping sites for photoexcited conduction band electrons. As one might expect, the  $\text{Er}^{3+}$  dopant gives rise to additional deep traps, which may be responsible for the observed “trap-to-trap hopping”<sup>31,32</sup> of the photoexcited conduction band electrons. This gives rise to a fast trapping process on the 360 fs time scale and a slower trapping component of 100 ps lifetime. Less obvious is the fact that the trapping to dopant sites can be largely circumnavigated by adding efficient electron acceptors on the nanocrystal interface. This was accomplished with BQ, which removed the photoexcited electron from the initially populated dopant-induced defect sites. The back electron transfer from the electron acceptor anion to the hole on the nanocrystal, is intercepted by low-lying trap sites. This allows an estimate of the redox potential of the trapping sites, which must be lower than that of the electron acceptor (BQ:  $-0.45$  V versus SCE) in this system.

## 3. Si NCs with an Er-enriched surface layer

The femtosecond spectroscopic measurement of the erbium surface-enriched system, presented in Fig. 6, shows again the formation of a broad transient absorption with no distinct features, as in the system with no erbium dopant. But, as in the case of the randomly dispersed erbium-doped nanocrystals, two trapping components with lifetimes of 2.4 and 182 ps were observed, indicative of a trap-to-trap hopping mechanism.

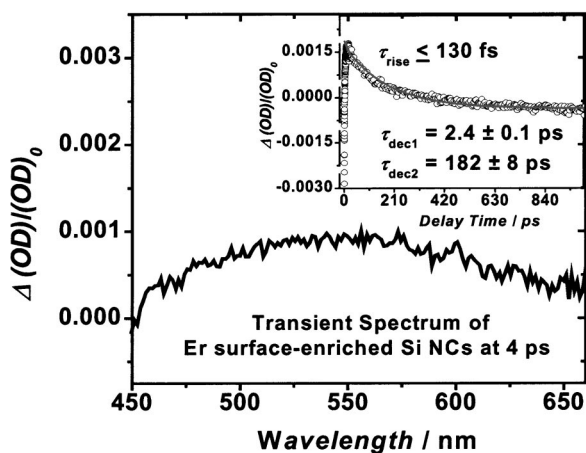


FIG. 6. Femtosecond transient absorption of Si NCs with an Er-enriched surface layer after excitation with 390 nm laser pulses. The inset shows the kinetics observed for the transient absorption at 550 nm.

Addition of BQ to the erbium surface-enriched nanocrystal system leads to the formation of the charge transfer state within 214 fs. The charge transfer state ( $\text{Si NC}^+\text{BQ}^-$ ) as in the previous cases is characterized by the superposition of the transient spectra on  $\text{BQ}^-$  anion around 500 nm and the partial bleach of the nanocrystal absorption at longer wavelengths (Fig. 7).

#### IV. DISCUSSION

The parameters characterizing the early time relaxation dynamics in the investigated Si nanocrystals are summarized in Table I. Comparison of the trapping times of the undoped Si NCs with the sample possessing randomly dispersed  $\text{Er}^{3+}$  centers, indicates that the trapping probability for the investigated system is greatly increased with the addition of  $\text{Er}^{3+}$ . The incorporation of  $\text{Er}^{3+}$  ions into the core of the nanocrystals appears to open up additional nonradiative relaxation pathways, which greatly shortens the fastest trapping time component of the conduction band electrons from 134 ps to

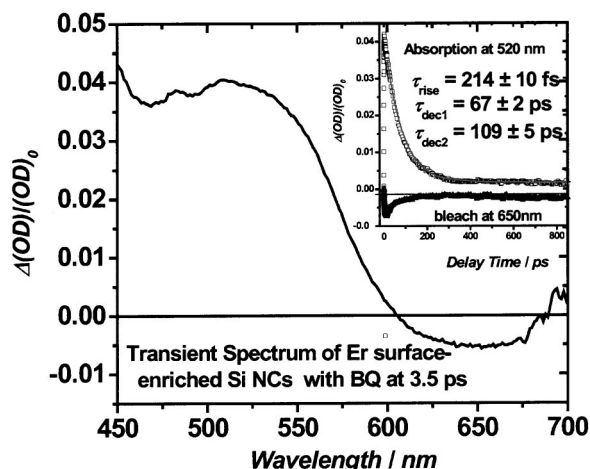


FIG. 7. Femtosecond transient absorption of  $\text{Er}^{3+}$  surface-enriched Si NCs with BQ adsorbed on the surface after excitation with 390 nm pulses. The inset shows the kinetics observed for the transient absorption at 520 nm and the transient bleach at 650 nm.

360 fs in the doped nanocrystals. Similarly, the erbium surface-enriched nanocrystals exhibit a faster electron trapping time of 2.4 ps compared to the undoped Si NCs. It is also noteworthy to mention the presence of an additional trapping relaxation process with a lifetime of 100 ps for the internally erbium-doped Si nanocrystal sample and 182 ps for the surface-enriched sample. Addition of the BQ to the nanocrystal samples reveals that the fastest electron transfer occurs in the undoped Si nanocrystal sample, and is longer for the erbium-doped samples. This observation indicates the relative depth of the trapping sites in the erbium-doped samples. Assuming that the excited-state electron transfer is an activated process, the different rise times could result from the different depths of the initial electron traps. Two aspects of the early time relaxation dynamics of the investigated Si nanocrystals is of considerable interest and will be addressed in the following section: First, the effect of erbium doping on the nonradiative relaxation pathways of the photoexcited electrons in Si nanocrystals, and second, the influence of the erbium architecture on the carrier dynamics.

#### A. Influence of the erbium dopant on the electron relaxation dynamics

The undoped Si nanocrystals show a sufficient density of trapping sites such that trap state absorption is the dominant transient feature after femtosecond laser excitation. In general, the introduction of  $\text{Er}^{3+}$  centers adds other significant trapping sites to the nanocrystal and is responsible for the efficient trap state population and the corresponding transient trap state absorption. Based on analogies with  $\text{Er}^{3+}$  ions implanted into bulk Si, it is likely that the electrons are not actually trapped on  $\text{Er}^{3+}$  sites but rather that the dopant induces other defect sites in the crystal that are populated. This is consistent with the obtained HRTEM images obtained for the Si nanocrystals, which indicates a great number of dislocations and stacking fault defects in the crystal lattice of the doped nanocrystals. This phenomenon may help explain the additional electron trapping processes that are observed in the doped nanocrystals.

Upon photoexcitation of the randomly dispersed erbium-doped Si nanocrystal sample, the conduction band electron is very quickly localized within 220 fs to a shallow trap. A subsequent transport to a deeper trap with a lifetime of 100 ps is then observed, indicative of a possible trap-to-trap electron hopping mechanism. This type of mechanism has been proposed for semiconductor systems with a substantial number of defect sites,<sup>31,32</sup> which is likely the case for the investigated erbium-doped nanocrystal samples. The photoexcited electron will remain in the traps until recombination with a hole will occur. In the case of an indirect bandgap material such as Si, the recombination process is phonon assisted. However, with the addition of erbium centers the number of deep traps increases, resulting in additional nonradiative relaxation pathways which shorten the lifetime of the photoexcited electron. As a consequence, the erbium-induced defect sites help promote the electron-hole recombination by providing a fast nonradiative route for the electron to hop from trap to trap site until it undergoes radiative or nonradiative

TABLE I. Early time relaxation dynamics in silicon nanocrystals.

Nanocrystal type	Trap state lifetime(s)		BQ charge transfer	
	Risetime $\tau_{\text{rise}}$ /Lifetime(s) $\tau_{\text{dec}}$		Risetime/Lifetime(s) $\tau_{\text{dec}}$	
Undoped Si NCs	$\leq 130$ fs <sup>a</sup>	$134 \pm 7$ ps	$150 \pm 30$ fs	$36 \pm 2$ ps (58%) $130 \pm 9$ ps (42%) Avg.: 75 ps
Randomly dispersed Er-doped Si NCs	$\leq 130$ fs <sup>a</sup>	$360 \pm 30$ fs $100 \pm 9$ ps	$220 \pm 12$ fs	$40 \pm 1$ ps (66%) $165 \pm 6$ ps (34%) Avg.: 82.5 ps
Surface Er-doped Si NCs	$\leq 130$ fs <sup>a</sup>	$2.4 \pm 0.1$ ps $182 \pm 8$ ps	$214 \pm 10$ fs	$67 \pm 2$ ps (85%) $109 \pm 5$ ps (15%) Avg.: 73.3 ps

<sup>a</sup>Rise of the signal within the excitation laser pulse.

recombination with the hole. Thereby, energy transfer to the  $\text{Er}^{3+}$  center can occur.

The presence of low-lying trap sites in the doped Si sample is further confirmed with the addition of BQ of the surface of the nanocrystals. The back electron transfer seems not to recover completely to the ground state in the doped Si NCs. Instead of the electron–hole recombination, the electrons appear to be captured at deep trap states hindering the complete recovery of the NC ground state and its spectrum.

For these studies BQ was the molecule chosen because it is well known as an electron acceptor molecule. In addition, from previous work we have discovered via FT-infrared spectroscopy that BQ binds directly to the semiconductor NC surface via its oxygen electrons (lone pairs).<sup>29</sup> This direct surface adsorption is responsible for the observed ultrafast electron transfer process. Furthermore, the redox potential for BQ is well documented ( $-0.45$  V versus SCE)<sup>33</sup> and allows a relative estimation of the energy levels of the initial trapping sites in the doped and undoped NCs (Fig. 8).

### B. Influence of $\text{Er}^{3+}$ architecture on the electron dynamics

A close comparison of the trap state lifetimes of the erbium surface-enriched with that of the internally doped Si nanocrystals shows considerably shorter lifetimes for the latter. This observation leads to the conclusion that  $\text{Er}^{3+}$  in the surface-enriched Si NCs has a different effect on the conduction band electron dynamics than when the dopant is randomly dispersed throughout the Si lattice. The trapping pro-

cesses in the internally doped nanocrystal sample seems to be more favorable and lead to faster trapping times (100 ps compared to 182 ps).

The data also suggest that the charge transfer complex formed between the nanocrystal and the electron acceptor BQ possesses a longer rise time than when the  $\text{Er}^{3+}$  centers are randomly dispersed throughout the nanocrystal than when clustered at the surface, thereby indicating that there are deeper trap states initially occupied in the internally doped nanocrystals compared to the undoped and surface-doped Si NCs. Furthermore, the back electron transfer lifetimes are longer in the core-doped nanocrystals, which confirms the presence of low-lying trap sites that favor the interception of the returning electron. These observations are also consistent with the near infrared photoluminescence mechanism of each type of Si nanocrystal (Fig. 9). Previous measurements have shown that the internally Er-doped material emits at 1540 nm. This is attributed to an excitation pathway involving energy transfer from the recombination process of the photoexcited carriers at an interfacial site. Efficient energy transfer requires resonance between the electron–hole recombination process and the  $\text{Er}^{3+}$  excited state. This is consistent with the presence of low-lying trap states in the internally doped Si nanocrystal sample. On the other hand, the lack of emission in the surface-enriched sample can simply mean that high local concentrations of  $\text{Er}^{3+}$  ions can result in a co-operative upconversion, in which an  $\text{Er}^{3+}$  ion de-excites by transferring its energy to a neighboring excited ion, promoting it into higher energy levels.

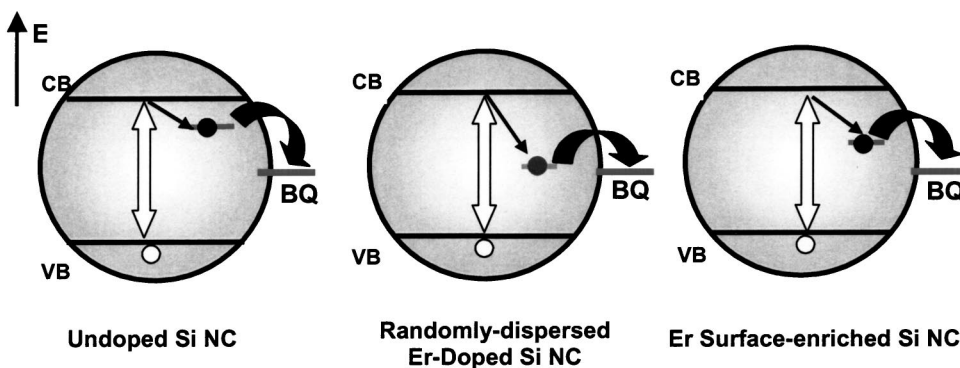


FIG. 8. Schematic diagram of the electron transfer process to benzoquinone (BQ) across the surface of Si nanocrystals.

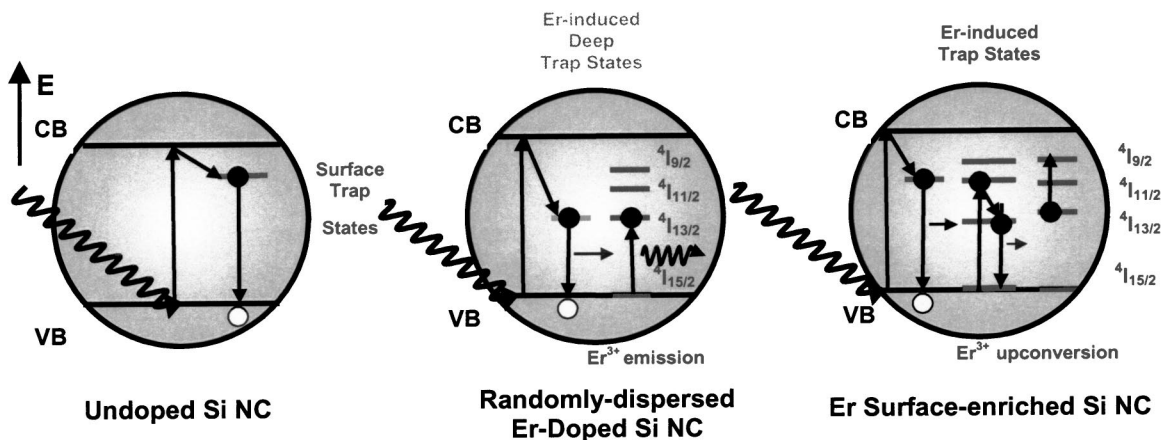


FIG. 9. Schematic diagram of the different relaxation processes in Si nanocrystals.

In addition, the forward electron transfer rate to BQ gives interesting insights into the effect of  $\text{Er}^{3+}$  doping on the energy level structure of the NC. Here, we observe that the change in forward electron transfer rates (from 150 to 220 fs) indicate that there could be an ultrafast electron trapping process occurring in the  $\text{Er}^{3+}$  doped NCs, consistent with the overall slower forward electron transfer of the doped systems. Moreover, it was shown that the internal doping has a greater effect than the surface doping in the Si NCs. This could imply a stronger lattice distortion and deeper defect formation for internal doping compared to surface doping (see Table I). In a similar way one could explain the different CT lifetimes. The randomly dispersed erbium-doped NCs show longer back electron transfer times, possibly because low-lying trapping sites could intercept the back electron transfer and cause the electron/hole recombination rate to slow down. The presented results may explain the observed emission in internally doped NCs and the lack thereof in surface-doped ones. In internally doped Si NCs, the excited electrons get trapped faster and efficiently relax into lower lying trapping sites, which then allow the observed resonance energy transfer to the  $\text{Er}^{3+}$  dopant.

## V. CONCLUSION

Femtosecond time-resolved transient absorption spectroscopy is a valuable tool in elucidating the early relaxation dynamics in Si nanocrystals. Analysis of the transient absorption spectra of the three Si nanocrystal samples reveals the presence of additional deep trap states upon incorporation of erbium into the Si host. The increase in number of defect sites upon addition of erbium promotes an electron trap-to-trap hopping mechanism that eventually facilitates the faster recombination of the photogenerated electron with the hole. Comparison of the trap state lifetimes of the Si NCs with randomly dispersed  $\text{Er}^{3+}$  centers with that having an Er-enriched surface layer show an effect of the erbium-dopant architecture on the electron relaxation dynamics. The trapping process seems to be more efficient when  $\text{Er}^{3+}$  ions are dispersed in the core of the nanocrystals, which may help explain the observation of emission in the erbium-doped nanocrystals.

Addition of the electron acceptor, BQ, on the surface of the Si nanocrystal samples provides a method for assessing the relative depths of the trapping sites in the investigated system. Analysis of the charge transfer rise time and the subsequent back electron transfer to the NCs supports the presence of low-lying trap states in the erbium-doped Si nanocrystals.

## ACKNOWLEDGMENTS

C.B. would like to acknowledge financial support by NSF (No. CHE-0239688), ACS-PRF and the Ohio Board of Regents. J.C. gratefully acknowledges the National Science Foundation and the Robert A. Welch Foundation for financial support of this research.

- <sup>1</sup>H. Ennen, J. Schneider, G. Pomrenke, and A. Axman, *Appl. Phys. Lett.* **43**, 943 (1983).
- <sup>2</sup>G. Franzò, V. Vinciguerra, and F. Priolo, *Appl. Phys. A: Mater. Sci. Process.* **69**, 3 (1999).
- <sup>3</sup>M. Fujii, M. Yoshida, Y. Kanazawa, S. Hayashi, and K. Yamamoto, *Appl. Phys. Lett.* **71**, 1198 (1997).
- <sup>4</sup>A. J. Kenyon, P. F. Trwoga, M. Federighi, and C. W. Pitt, *J. Phys.: Condens. Matter* **6**, L319 (1994).
- <sup>5</sup>A. Polman, *J. Appl. Phys.* **82**, 1 (1997).
- <sup>6</sup>J. Michel, L. V. C. Assali, M. T. Morse, and L. C. Kimerling, *Semicond. Semimetals* **49**, 111 (1998).
- <sup>7</sup>S. Coffa, G. Franzò, F. Priolo, A. Polman, and R. Serna, *Phys. Rev. B* **49**, 16313 (1994).
- <sup>8</sup>J. Palm, F. Gan, B. Zheng, J. Mitchel, and L. C. Kimerling, *Phys. Rev. B* **54**, 17603 (1996).
- <sup>9</sup>D. Pacifici, A. Irrera, G. Franzò, M. Miritello, F. Iacona, and F. Priolo, *Physica E* **16**, 331 (2003).
- <sup>10</sup>A. J. Kenyon, C. E. Chryssou, C. W. Pitt, T. Shimizu-Iwayama, D. E. Hole, N. Sharma, and C. J. Humphreys, *J. Appl. Phys.* **91**, 367 (2002).
- <sup>11</sup>S. Lombardo, S. U. Campisano, G. N. van den Hoven, A. Cacciato, and A. Polman, *Appl. Phys. Lett.* **63**, 1942 (1993).
- <sup>12</sup>H. S. Han, S. Y. Seo, and J. H. Shin, *Appl. Phys. Lett.* **79**, 4568 (2001).
- <sup>13</sup>*Frontiers of Nano-Optoelectronic Systems, NATO Science Series*, edited by L. Pavesi and E. Buzaneva (Kluwer Academic, New York, 2000), Vol. 6, p. 99.
- <sup>14</sup>G. Franzò, F. Iacona, V. Vinciguerra, and F. Priolo, *Mater. Sci. Eng., B* **69/70**, 338 (1999).
- <sup>15</sup>V. Vinciguerra, G. Franzò, F. Priolo, F. Iacona, and C. Spinella, *J. Appl. Phys.* **87**, 8165 (2000).
- <sup>16</sup>J. V. St. John, J. L. Coffer, Y. Chen, and R. Pinizzotto, *J. Am. Chem. Soc.* **121**, 1888 (1999).

- <sup>17</sup>J. St. John, J. Coffey, Y. Chen, and R. Pinizzotto, *Appl. Phys. Lett.* **77**, 1635 (2000).
- <sup>18</sup>R. Senter, Y. Chen, J. Coffey, and L. Tessler, *Nanolett.* **1**, 383 (2001).
- <sup>19</sup>J. V. St. John and J. L. Coffey, *J. Phys. Chem. B* **105**, 7599 (2001).
- <sup>20</sup>J. Ji, Y. Chen, R. A. Senter, and J. L. Coffey, *Chem. Mater.* **13**, 4783 (2001).
- <sup>21</sup>L. R. Tessler, J. L. Coffey, J. Ji, and R. A. Senter, *J. Non-Cryst. Solids* **299–302**, 673 (2002).
- <sup>22</sup>A. Mourchid, R. Vanderhaghen, D. Hulin, and P. M. Fauchet, *Phys. Rev. B* **42**, 7667 (1990).
- <sup>23</sup>P. M. Fauchet and D. Hulin, *J. Opt. Soc. Am. B* **6**, 1024 (1989).
- <sup>24</sup>V. Klimov, D. McBranch, and V. Karavanskii, *Phys. Rev. B* **52**, 16989 (1995).
- <sup>25</sup>V. I. Klimov, V. S. Dneprovskii, and V. A. Karavanskii, *Appl. Phys. Lett.* **64**, 2691 (1994).
- <sup>26</sup>R. Tomasiunas, I. Pelant, J. Koka, P. Knápek, R. Lévy, P. Gilliot, J. B. Grun, and B. Hönerlage, *J. Appl. Phys.* **79**, 2481 (1996).
- <sup>27</sup>K. Littau, P. Szajowski, A. Muller, A. Kortan, and L. Brus, *J. Phys. Chem. B* **97**, 1224 (1993).
- <sup>28</sup>Y. Lou, X. Chen, A. C. S. Samia, and C. Burda, *J. Phys. Chem. B* **107**, 12431 (2003).
- <sup>29</sup>C. Burda, T. C. Green, S. Link, and M. A. El-Sayed, *J. Phys. Chem. B* **103**, 1783 (1999).
- <sup>30</sup>T. Shida, *Electronic Absorption Spectra of Radical Anions* (Elsevier, Amsterdam, 1988).
- <sup>31</sup>B. I. Shklovskii and A. L. Efros, *Electronic Properties of Doped Semiconductors* (1984).
- <sup>32</sup>J. J. Cavaleri, D. E. Skinner, D. P. Colombo, Jr., and R. M. Bowman, *J. Chem. Phys.* **103**, 5378 (1995).
- <sup>33</sup>S. L. Murov, *Handbook of Photochemistry* (Dekker, New York, 1973).